Chapter 7

CONCLUSION

7.1 Summary of this thesis

The methodology presented in this thesis is unique in its character: it allows for the simultaneous and global measurement of the temperature and the solar wind velocity in the solar corona. This line of thinking originated from Cram's (1976) theoretical formulation for the formation of the K-corona and its properties. The physical properties that were taken into consideration in the formulation of the theory included the effects due to thermal Doppler broadening, limb darkening effects, angular dependence of the Thomson scattering and the cumulative contribution from different positions along the line of sight. The properties that were derived were the existence of temperature sensitive anti-nodes in the K-coronal spectrum and the remarkable independence of the temperature insensitive nodes with height above the solar limb. It was suggested that these properties could be exploited to measure the coronal temperature from the K-coronal intensity profile. Ichimoto et al. (1996) demonstrated the feasibility of Cram's method by analyzing the K-coronal spectrum obtained using a slit spectrograph during the total solar eclipse of 3 November 1994 in Putre, Chile.

In this thesis Cram's theory was extended by including the effects of coronal expansion in the formation of the K-corona. While confirming the properties derived by Cram, an additional property was discovered with the introduction of the solar wind. This allows for the **simultaneous** determination of both the **temperature** and the **wind velocity** from the same K-coronal spectral measurement. An overview of the theory and of the method can be found in chapters-**1** and **2**. The dependence of the theoretical model on the selection of the electron number density model, different temperature and wind profiles and the numerical procedures are discussed in chapter-**5**.

In this thesis, instead of a slit spectrograph a fiber optic spectrograpgh was designed whose features allowed for **global** determination of the K-coronal spectra all around the solar limb and at different heights. The instrument is discussed in chapter-**3**. Combining the theoretical prediction on the feasibility to determine both the temperature and the wind velocity from a single K-coronal spectrum and the instruments ability to globally measure the K-coronal spectra, the instrument was named **MACS** for Multi Aperture Coronal Spectrometer. The very first effort of its kind was tested in conjunction with the total solar eclipse of 11 August 1999 in Elazig, Turkey. The observational results are discussed in chapter-**4**. We were successful in determining the electron temperature at various points in the inner corona.

However, an important (and unwelcome) aspect of our observations concerns the degradation of the data due to instrumental scattering. Because of unexpectadly high

levels of scattering, we were not successful in obtaining reliable estimates of wind velocity. Although remedial measures were taken in expectation of possible instrumental scattering, the actual magnitude of the scattered light was not realized. Our efforts to reduce scattering were compounded by the inability to replicate the observing conditions in a laboratory and the lack of funds to obtain high quality optical components. One of the vital ingredient required to minimize instrumental scattering is careful selection of high quality optical components. Another important feature for the success of MACS would be to perform an absolute wavelength calibration in the laboratory. The extent of the instrumental scattering and some of the remedial measures are discussed in chapter-**6**.

Despite the lack of success in determining the wind velocity, our success in determining the coronal temperature using MACS has already been recognized as a successful proof-of-concept by a funding agency. A proposal to mate MACS concept with a coronagraph was submitted to NASA and it received favourable review. As a result, funds have been awarded for an upgraded version of our experiment in which the scattered light problem should be much reduced. It is hoped that the upgraded version of MACS will be ready for the solar eclipse of 21 June 2001 in Africa. At this eclipse MACS is to be complimented with a filter based system, where filters would be centered at the temperature and wind sensitive wavelength positions. The concept of MACS has also been recommeded as an instrument in the proposal for the instrumental package that would fly aboard the Solar Probe. A brief review of the Solar Probe is given in section (**7.2**).

7.2 Using a spacecraft platform

A space platform envisaged for implementing the theoretical concept of MACS is the unmanned Solar Probe Spacecraft that will approach the sun at four solar radii at its perihelion. In this proposal a series of filters centered on the temperature and the wind sensitive wavelength positions is proposed. This would allow for both temperature and wind velocity measurements.Figure (**7.1**) shows the parabolic path of Solar Probe.

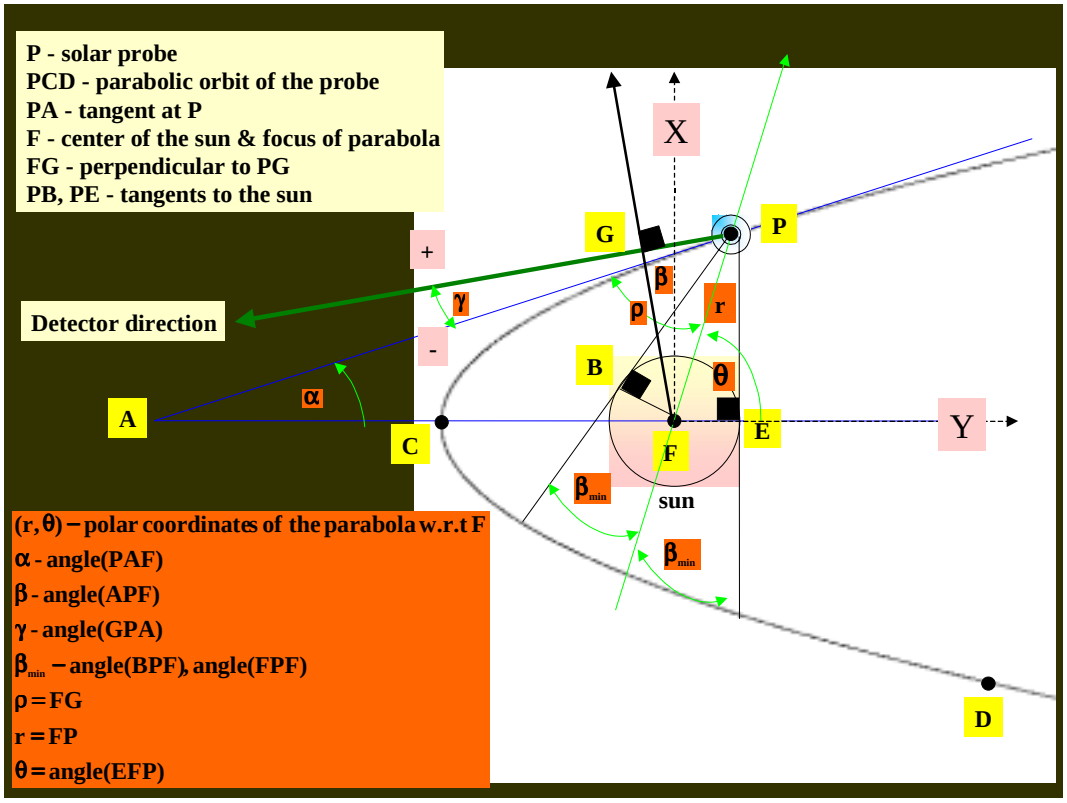

Figure (7.1). The path envisaged for the unmanned Solar Probe Spacecraft. At the perihelion (C) and the poles the spacecraft will be four and eight solar radii, respectively, from the center of the sun. The position of the spacecraft (P) is given by (r, θ) with respect to the center of the sun. In this picture the parabolic path, the detector plane and the center of the sun are in the same plane.

The equation of the parabolic orbit of the Solar Probe as depicted in figure (**7.1**) in polar coordinates is given by equation (**7.1**).

$$\mathbf{r(\theta) = \frac{2.0 \times FC}{1 - \cos(\theta)} = \frac{8.0R}{1 - \cos(\theta)}} \quad \textbf{(7.1)}$$

where R is the solar radius & FC = 4R

The angle α made by the tangent at P with the x-axis is given by equation (**7.2**).

$$\alpha = \tan^{-1}\left(\frac{1 - \cos(\theta)}{\sin(\theta)}\right) \quad \textbf{(7.2)}$$

The derivation of equation (**7.2**) is as follows.

$$y = r\sin(\theta) \rightarrow dy = r\cos(\theta)d\theta + \sin(\theta)dr$$

$$x = r\cos(\theta) \rightarrow dx = -r\sin(\theta)d\theta + \cos(\theta)dr$$

$$\frac{dy}{dx} = \frac{r\cos(\theta)d\theta + \sin(\theta)dr}{-r\sin(\theta)d\theta + \cos(\theta)dr} = \frac{r\cos(\theta) + \sin(\theta)(dr/d\theta)}{-r\sin(\theta) + \cos(\theta)(dr/d\theta)}$$

$$\textbf{from equation (1)}\ \frac{dr}{d\theta} = \frac{-2 \times FC \times \sin(\theta)}{(1 - \cos(\theta))^2}\ \textbf{\& using}\ r = \frac{2 \times FC}{1 - \cos(\theta)}$$

$$\tan(\alpha) = \frac{dy}{dx} = \frac{1 - \cos(\theta)}{\sin(\theta)}$$

From the triangle APE the relationship between α, β **and** θ is given by equation (**7.3**).

$$\theta = \alpha + \beta \rightarrow \beta = \theta - \alpha \quad \textbf{(7.3)}$$

Supposing the detector direction is γ degrees from the tangent to the orbit at position (**P**) then the perpendicular distance ρ from the center of the sun to the line of sight of the detector is given by equation (**7.4**).

$$\rho = r\sin(\beta + \gamma) \tag{7.4}$$

At this instance the distance between the spacecraft and the intersection between the line of sight and the normal from the center of the sun is given by equation (**7.5**).

$$PG = r\cos(\beta + \gamma) \tag{7.5}$$

In order to prevent the detector being pointed directly at the sun the angle γ will have to satisfy the following condition given by equation (**7.6**).

$$\begin{aligned} &\gamma_- > -(\beta - \beta_{min}) \text{ measured in the (-) direction} \\ &\gamma_+ < 2\pi - (\beta + \beta_{min}) \text{ measured in the (+) direction} \\ &\text{where } \beta_{min} = \sin^{-1}\left(\frac{R}{r}\right) \end{aligned} \tag{7.6}$$

In determining the theoretical K-coronal spectrum observed by the Solar Probe the only change occurs in the x-integration (along the line of sight) as shown in equation (**7.7**).

$$\int_{-\infty}^{+\infty} dx \rightarrow \int_{-PG}^{+\infty} dx \tag{7.7}$$

The above integration may be performed the following way as shown in equation (**7.8**). The first and the second integrations are performed using trapezoidal composite rule and Laguerre integration, respectively.

$$\int_{-PG}^{+\infty} f(x)dx = \int_{-PG}^{0} f(x)dx + \int_{0}^{+\infty} f(x)dx$$
$$= \int_{-PG}^{0} f(x)dx + \int_{0}^{+\infty} e^{-x}(f(x)e^{+x})dx$$
$$= \frac{h}{2}\left(2\times\sum_{i=0}^{20} f(z_i) - f(z_0) - f(z_{20})\right) + \sum_{i=0}^{20} w_i e^{+x_i} f(x_i)$$
$$\text{where } h = \frac{0 - (-PG)}{20} \;\&\; z_i = -PG + i\times h \qquad \textbf{(7.8)}$$

Figure (**7.2**) and figure (**7.3**) show for solar wind velocities 0.0 and 400.0 km/sec, respectively, the theoretical K-coronal intensity variation for various detector elevations with respect to the tangent when the spacecraft is positioned at the pole (P). Figure (**7.4**) shows the variation of the wind-sensitive intensity ratio against the detector tilt γ for various wind velocities at a constant temperature of 1.0 MK and the spacecraft positioned at the pole. Figure (**7.5**) shows the variation of the temperature-sensitive intensity ratio against the detector tilt γ for various temepratures at a constant wind velocity of 400.0 km/sec and the spacecraft positioned at the pole. Figures (**7.6**) and (**7.7**) show the variation of the temperature-sensitive intensity ratio against temperature for various wind velocities and the variation of the wind-sensitive intensity ratio against wind velocitiy for various temperatures, respectively, for a given detector tilt angle γ and the spacecraft positioned at the pole.

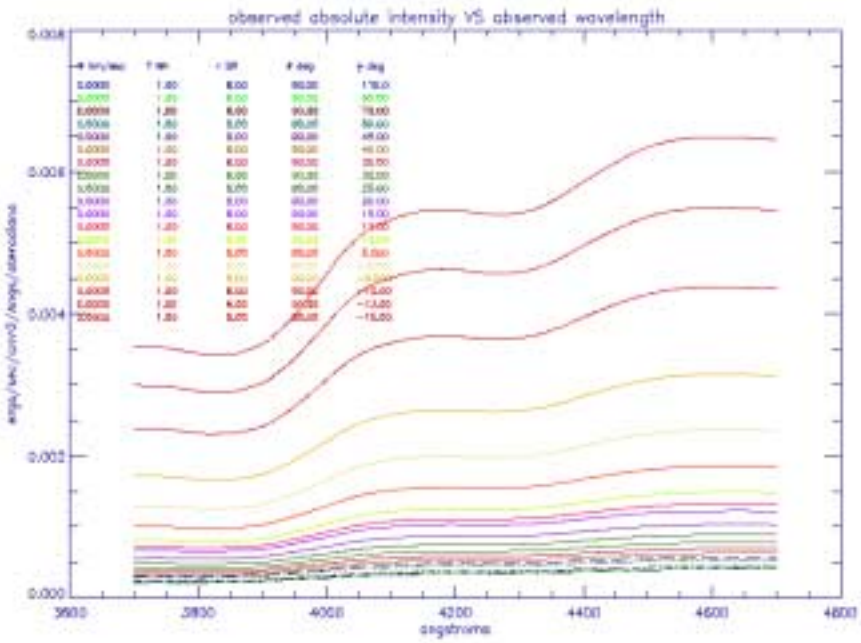

Figure (7.2) The theoretical K-coronal intensity variation for various detector elevations for 0.0 km/sec wind velocity and the spacecraft positioned at the pole (P).

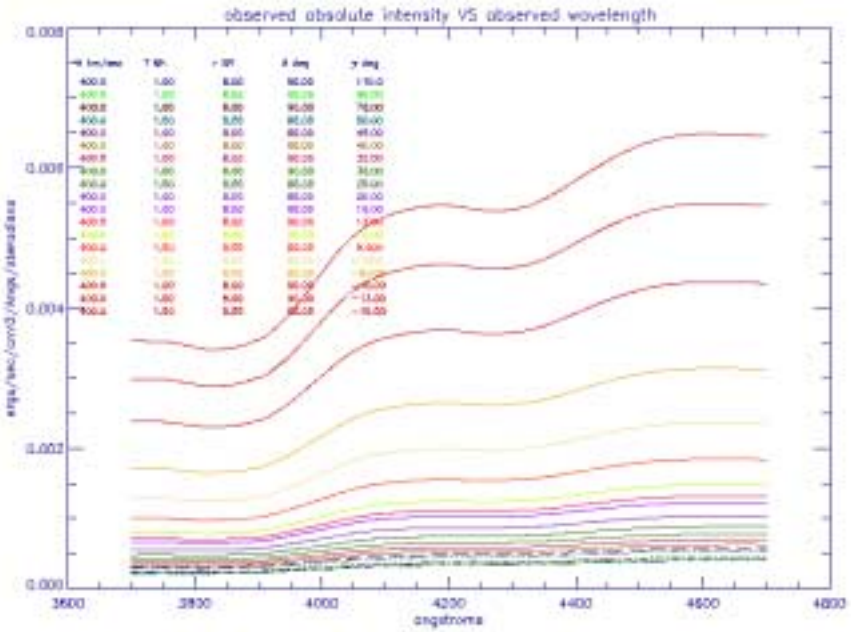

Figure (7.3). The theoretical K-coronal intensity variation for various detector elevations for 400.0 km/sec wind velocity and the spacecraft positioned at the pole (P).

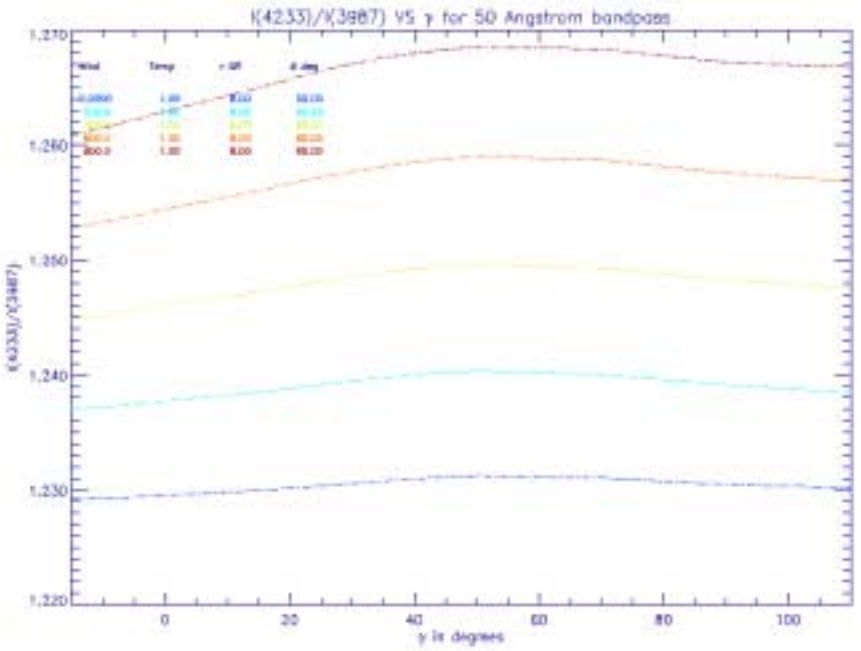

Figure (7.4). The variation of the wind-sensitive intensity ratio against γ for various wind velocities at T=1.0 MK and the spacecraft positioned at the pole.

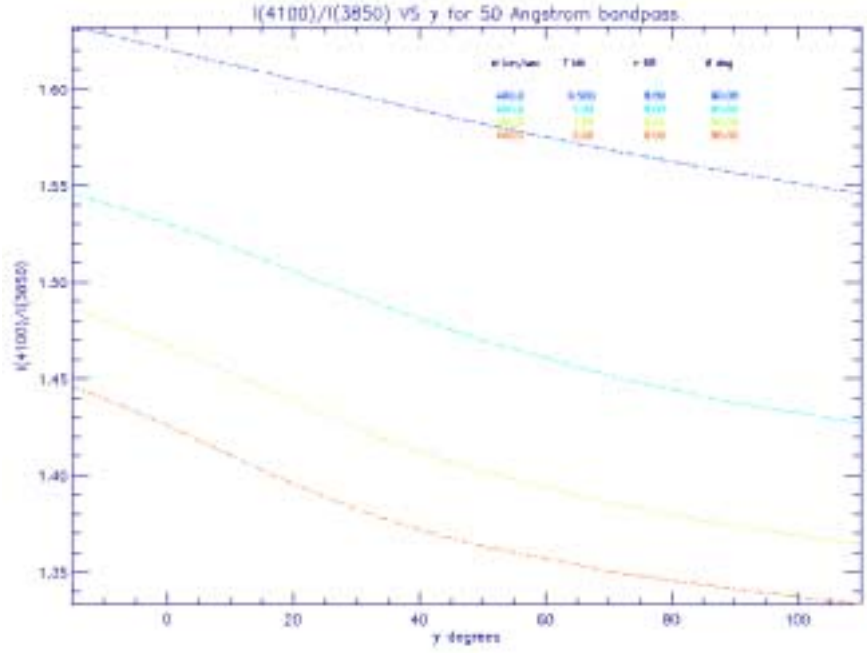

Figure (7.5). The variation of the temperature-sensitive intensity ratio against γ for various temperatures at W=400.0 km/sec and the spacecraft positioned at the pole.

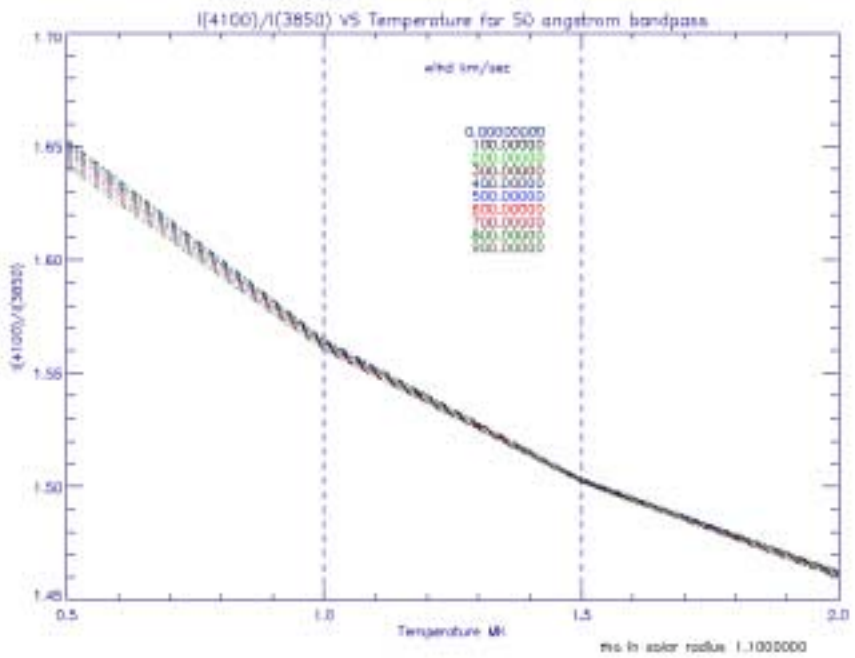

Figure (7.6). Temperature-sensitive intensity ratioVS Temperature for various wind velocities at γ = 0.0 degrees and the spacecraft positioned at the pole.

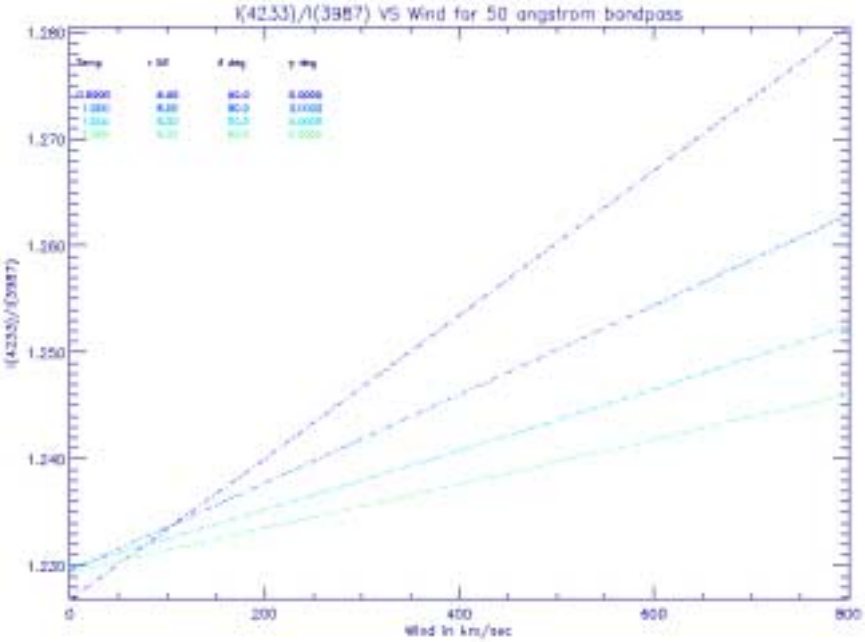

Figure (7.7). Wind-sensitive intensity ratioVS Wind velocity for various temperatures at γ = 0.0 degrees and the spacecraft positioned at the pole.

These plots show the promise behind the theoretical concept of MACS being employed from a space platform deep inside the solar corona for the measurement of the coronal temperature and the solar wind velocity thus avoiding the F-corona and the use of a coronagraph. Even the spectrograph could be avoided with the use of optical filters centered at the temperature and wind sensitive wavelengths. The temperature and wind sensitive intensity ratios remain almost the same even at fifty angstrom bandpass. Figures (**7.8**) and (**7.9**) show the temperature and wind sensitive intensity ratios, respectively, for the use of fiters centered at those wavelengths with a fifty angstrom bandpass for line of sight integration from $\pm\infty$ at 1.1 solar radii. This could be verified by the comparison of figures (**7.8**) and (**7.9**) with figures (**2.3**) and (**2.20**), respectively.

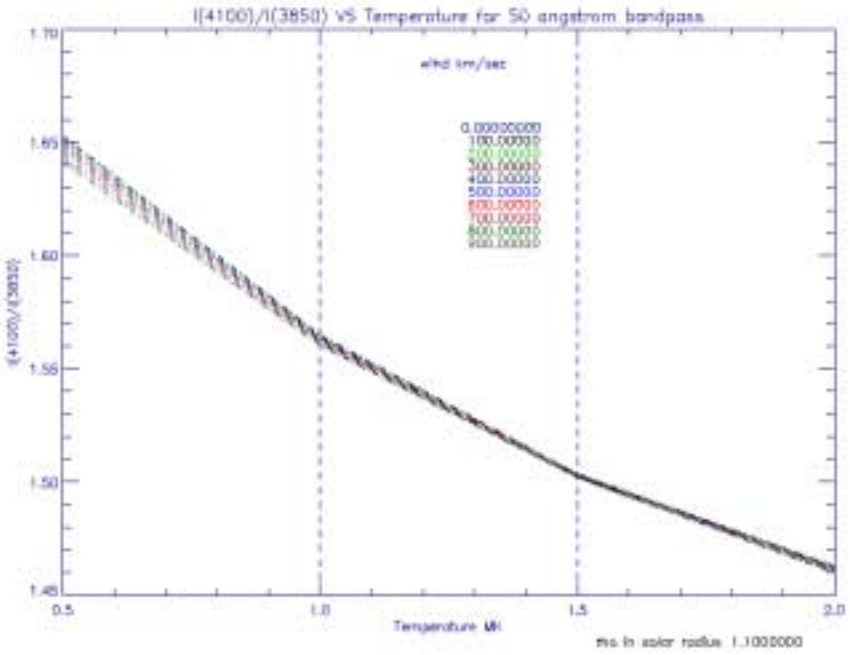

Figure (7.8). Temperature-sensitive intensity ratioVS Temperature for various wind velocities with intensities measured through filters of fifty angstrom bandpass centered at those wavelengths for line of sight at 1.1 solar radii.

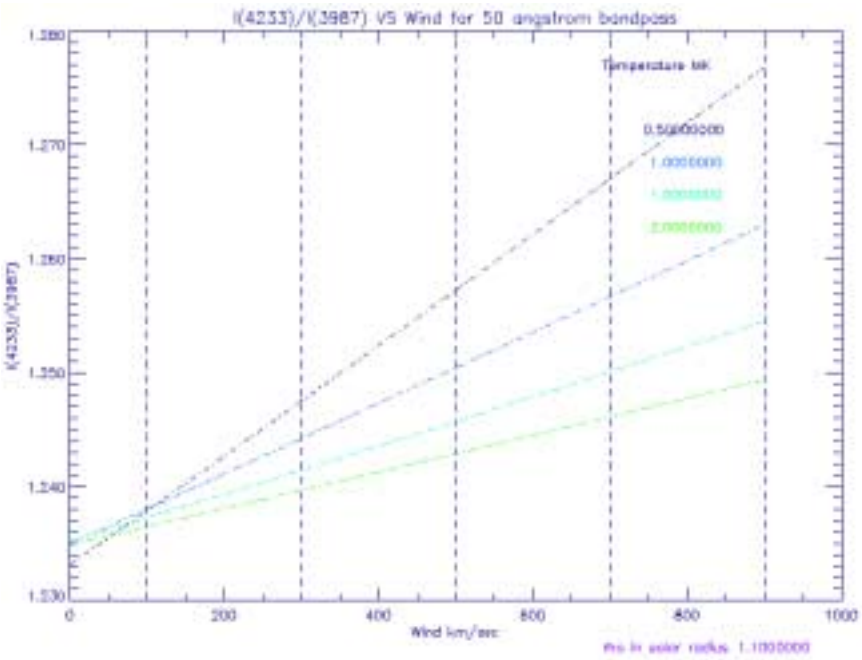

Figure (7.9). Wind-sensitive intensity ratioVS Wind velocities for various temperatures with intensities measured through filters of fifty angstrom bandpass centered at those wavelengths for line of sight at 1.1 solar radii.

In conclusion, with the approval of funding for a coronagraph for MACS the future is very optimistic as a tool for simultaneous and global coronal temperature and wind measurements. There is also good reason to hope that the concept can be applied as an instrument on a space-based platform.